

# SBDART: A Research and Teaching Software Tool for Plane-Parallel Radiative Transfer in the Earth's Atmosphere



Paul Ricchiazzi,\* Shiren Yang,\* Catherine Gautier,\*<sup>+</sup> and David Sowle<sup>#</sup>

## ABSTRACT

SBDART is a software tool that computes plane-parallel radiative transfer in clear and cloudy conditions within the earth's atmosphere and at the surface. All important processes that affect the ultraviolet, visible, and infrared radiation fields are included. The code is a marriage of a sophisticated discrete ordinate radiative transfer module, low-resolution atmospheric transmission models, and Mie scattering results for light scattering by water droplets and ice crystals. The code is well suited for a wide variety of atmospheric radiative energy balance and remote sensing studies. It is designed so that it can be used for case studies as well as sensitivity analysis. For small sets of computations or teaching applications it is available on the World Wide Web with a user-friendly interface. For sensitivity studies requiring many computations it is available by anonymous FTP as a well organized and documented FORTRAN 77 source code.

## 1. Introduction

The main driving force of the earth system is radiation forcing. The temperature and circulation of the earth atmosphere and surface are largely regulated by the amount of radiation the earth receives from the sun. The spectral composition of the radiation impacts life on earth through photosynthesis. Therefore, a detailed and quantitative knowledge of the earth radiation field is crucial to understand and predict the evolution of the components of the earth system. Until recently, the ability to compute detailed radiative quantities within the earth's atmosphere has been restricted to a relatively small group of researchers. The heavy investments of labor and computer time required to compile large molecular transmission data-

bases and perform lengthy multiple scattering radiative transfer computations put detailed radiative transfer (RT) computations out of reach of the general geoscience community. Within the last decade, however, the development of efficient radiative transfer algorithms and freely available gaseous transmission codes, coupled with the steady improvements in computer technology have made detailed atmospheric RT modeling accessible to a much larger audience. Now, with the addition of user-friendly interfaces, the models can be used as a teaching tool, making them even more broadly usable.

Radiative transfer computer codes, such as LOWTRAN (Kneizys et al. 1983) and MODTRAN (Berk et al. 1983), have provided an accurate and expedient way to compute radiation levels at low ( $20 \text{ cm}^{-1}$ ) and moderate ( $2 \text{ cm}^{-1}$ ) spectral resolution. LOWTRAN and MODTRAN were developed primarily to address the problem of computing the atmospheric transmission in clear sky conditions. Until recently, both codes used simple two-stream radiative transfer algorithms to handle multiple scattering in overcast conditions. Besides being less accurate than more sophisticated RT treatments, two-stream methods do not provide angular radiance information, a severe limitation particularly for the interpretation of satellite remote sensing observations. Because the

\*Institute for Computational Earth System Science, University of California, Santa Barbara, Santa Barbara, California.

<sup>+</sup>Geography Department, University of California, Santa Barbara, Santa Barbara, California.

<sup>#</sup>Mission Research Corporation, Santa Barbara, California.

Corresponding author address: Dr. Paul Ricchiazzi, Institute for Computational Earth System Service, University of California, Santa Barbara, Santa Barbara, CA 93106-3060.

E-mail: paul@icess.ucsb.edu

In final form 18 May 1998.

©1998 American Meteorological Society

LOWTRAN–MODTRAN codes were intended for a highly diverse audience, the input parameters describing cloud characteristics are rather generic. For example, though several cloud types can be specified, a full range of cloud characteristics is not available. This makes it difficult to perform sensitivity studies of such basic parameters as the mean cloud drop radius. Though a multistream RT treatment has been implemented in the most recent version of MODTRAN (Bernstein et al. 1996), the code inherits the same generic set of cloud models as earlier versions.

To improve on the LOWTRAN–MODTRAN treatment of the cloudy atmosphere and provide an easy-to-use comprehensive software tool, we have developed the SBDART (Santa Barbara DISORT Atmospheric Radiative Transfer) program. This FORTRAN computer program is designed for the analysis of a wide variety of radiative transfer problems encountered in satellite remote sensing and atmospheric radiation budget studies. The program is based on a collection of well tested and reliable physical models, which were developed by the atmospheric science community over the past few decades.

In developing SBDART, we have tried to follow modern standards of software design. The code structure is modular and excessive use of FORTRAN common blocks has been avoided. The routines, which cover a fairly wide variety of topics in atmospheric physics and radiative transfer, include ample documentation describing purpose, methodology, and input–output quantities. In addition to easing maintenance of the code, this approach provides a good starting point for researchers interested in using the routine library to develop their own RT codes or atmospheric science teachers interested in showing how radiation interacts with the atmosphere and surface properties. We have taken advantage of this foundation in the development of a separate 3D Monte Carlo RT model, which we have used to stimulate horizontal cloud heterogeneity (O’Hirok and Gautier 1998).

The remainder of this paper is organized as follows. In section 1 we discuss the key components of SBDART and the models on which they are based. Next, in section 2, we compare SBDART predictions to recently available measurements of long and short-wave (SW) radiation. A presentation of the Web version and discussion of its different uses is provided in section 3. We conclude in section 4 with several examples of research and instructional applications of SBDART.

## 2. Physical models

### a. *Standard atmospheric profiles*

We have adopted six standard atmospheric profiles that are intended to model the following prototypical climatic conditions: tropical, midlatitude summer, midlatitude winter, subarctic summer, subarctic winter, and US62, which represents typical conditions over the continental United States. These model atmospheres (McClatchey et al. 1972) have been widely used in the atmospheric research community and provide standard vertical profiles of pressure, temperature, water vapor, and ozone density. In addition, users may specify their own model atmosphere based on, for example, a series of radiosonde profiles. The concentration of trace gases such as CO<sub>2</sub> or CH<sub>4</sub> are assumed to make up a fixed fraction (that may be specified by the user) of the total particle density.

### b. *Standard ground reflectance models*

The ground surface cover is an important determinant of the overall radiation environment. In SBDART five basic surface types—ocean water (Tanre et al. 1990), lake water (Kondratyev 1969), vegetation (Reeves et al. 1975), snow (Wiscombe and Warren 1980)—and sand (Staetter and Schroeder 1978), are used to parameterize the spectral albedo of the surface, which is defined as the ratio of upwelling to downwelling spectral irradiance at the surface. The spectral albedo describing a given surface is often well approximated by combinations of these basic surface types. Input parameters in SBDART allow the user to specify a mixed surface consisting of weighted combinations of water, snow, vegetation, and sand. For example, a combination of vegetation, water, and sand can be adjusted to generate a new spectral reflectivity representing new/old growth, or deciduous versus evergreen forest. Combining a small fraction of the spectral reflectivity of water with that of sand yields an overall spectral dependence close to wet soil.

In SBDART we assume that the angular distribution of surface-reflected radiation is completely isotropic, irrespective of solar zenith angle. This Lambertian reflection assumption is probably adequate for most situations and is a convenient choice considering the scarcity of angular reflection data. However, it should be noted that large deviations from Lambertian reflection may occur, especially at shallow viewing and illumination angles, or when viewing a water surface at the specular angle (sun glint). We intend to implement nonisotropic reflection models as

more observational data of the bidirectional reflection distribution function become available.

### c. Scattering by cloud droplets

Clouds are a major modulator of the earth's climate, both by reflecting visible radiation back to space and by intercepting part of the infrared radiation emitted by the earth and reradiating it back to the surface. The computation of radiative transfer within a cloudy atmosphere requires knowledge of the extinction efficiency  $Q_{\text{eff}}$ , the single scattering albedo  $\omega$ , and the asymmetry factor  $g$ . The single-scattering albedo is the probability that an extinction event scatters rather than absorbs a photon. The asymmetry factor indicates the strength of forward scattering. We have computed these parameters using a Mie scattering code (Stackhouse 1991, personal communication) for spherical cloud droplets with a statistical distribution of drop radius. The radius distribution is given by a modified gamma size distribution:

$$N(r) = C(r/R_{\text{eff}})^{(p-1)}e^{-(p+2)r/R_{\text{eff}}}, \quad (1)$$

where  $C$  is a normalization constant,  $p$  is a dimensionless parameter that controls the width of the distribution, and  $R_{\text{eff}}$  is the effective radius. The effective radius is defined as the ratio of the third and second moments of the radius distribution. SBDART contains precomputed scattering parameters for a set of effective radii in the range 2 to 128  $\mu\text{m}$ . All distributions have width parameter,  $p = 7$ . Figure 1 shows the computed scattering parameters using this code. These results agree very well with the scattering parameters generated with Wiscombe's (1980) Mie code. To allow analysis of radiative transfer through cirrus clouds we also include the scattering parameters for spherical ice grains of a single-size distribution [given by Eq. (1)] with  $R_{\text{eff}} = 106 \mu\text{m}$ .

### d. Molecular absorption

SBDART relies on low-resolution band models developed for the LOWTRAN 7 atmospheric transmission code (Pierluissi and Peng 1985). These models provide clear-sky atmospheric transmission from 0 to 50 000  $\text{cm}^{-1}$  and include the effects of all radiatively active molecular species found in the earth's atmosphere. The models are derived from detailed line-by-line calculations that are degraded to 20  $\text{cm}^{-1}$  resolution for use in LOWTRAN. This translates to a wavelength resolution of about 5 nm in the visible and about 200 nm in the thermal infrared.

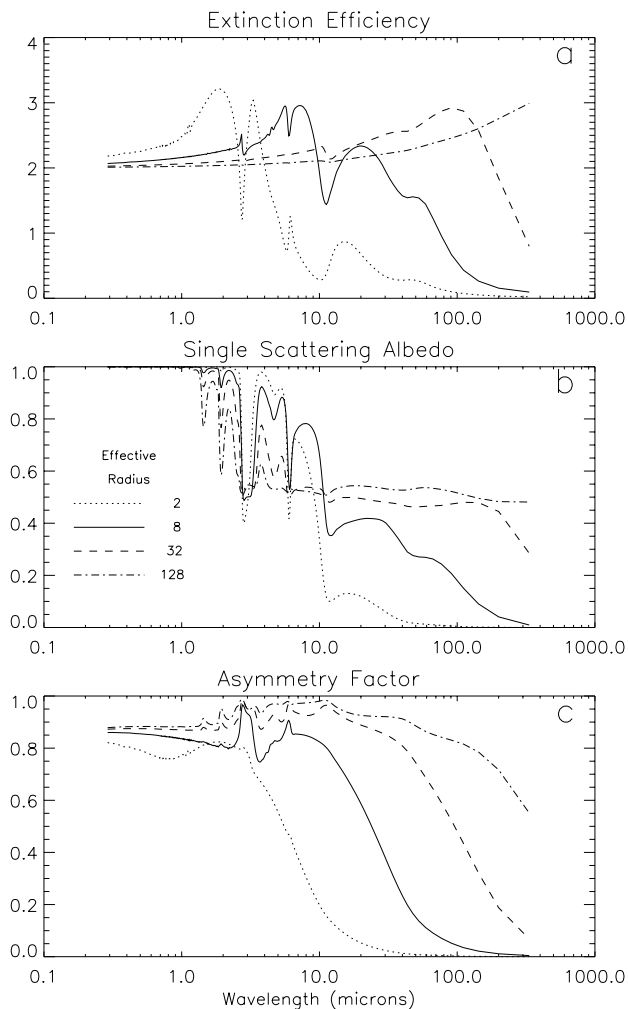


FIG. 1. Extinction efficiency (a), single-scattering albedo (b), and asymmetry factor (c) for cloud droplets of effective radius 2, 8, 32, and 128  $\mu\text{m}$ .

These band models represent rather large wavelength bands, and the transmission functions do not necessarily follow Beers Law. This means that the fractional transmission through a slab of material depends not only on the slab thickness, but also on the amount of material penetrated before entering the slab. Since the radiative transfer equation solved by SBDART assumes Beers Law behavior, it is necessary to express the transmission as the sum of several exponential functions (Wiscombe and Evans 1977). SBDART uses a three-term exponential fit, which was also obtained from LOWTRAN 7. Each term in the exponential fit implies a separate solution of the radiation transfer equation. Hence, the RT equation solver only needs to be invoked three times for each spectral increment. This is a great computational economy compared to a higher order fitting poly-

mial, but it may also be a source of significant error. However, since recent attempts to validate the predictions of radiation models in cloudy atmospheres have shown unexplained anomalous absorption (Zhang et al. 1997; Valero et al. 1997), it seems appropriate to delay implementation of an improved model until a better understanding of nonconservative scattering in the atmosphere is attained.

*e. Standard aerosol models*

Atmospheric aerosols affect the earth's energy balance primarily through scattering and absorption of SW radiation and through modification of cloud microphysics. For example, it has been postulated that anthropogenic sulfate aerosols may reduce the surface insolation sufficiently to partially offset the effects of increasing levels of greenhouse gases (Schwartz 1996). Aerosols may also have a strong indirect influence on the radiation budget. A large density of small aerosol particles can enhance cloud reflectivity in the SW by increasing the droplet number density for the same total amount of liquid water. Due to a lack of information on their global distribution, aerosols are considered a major uncertainty in climatic global change.

SBDART can compute the radiative effects of several lower- and upper-atmosphere aerosol types. In the lower atmosphere, typical rural, urban, or maritime conditions can be simulated using the standard aerosol models of Shettle and Fenn (1975). These models differ from one another in the way their extinction efficiency  $Q_{ext}$ , single-scattering albedo  $\omega$ , and asymmetry factor  $g$ , vary with wavelength and to the extent the scattering parameters depend on the surface relative humidity. Figure 2 shows the spectral variation of  $Q_{ext}$ ,  $\omega$ , and  $g$  for the urban aerosol model. The single-scattering albedo of this model shows a sensitivity to surface humidity greater than that of the other models. The maritime model, shown in Fig. 3, has weaker variation of "omega" with humidity, but a greater sensitivity of  $Q_{ext}$ . These differences follow from the particle-size distributions and the refractive properties of the aerosol constituents that are thought to be present at any given relative humidity. For example, the increase of urban single-scattering albedo with increasing humidity is caused by a relative reduction of the soot content as the aerosol particles take on more liquid water.

The total vertical optical depth of lower-atmosphere aerosols is derived from user-specified horizontal meteorological visibility,  $V$ , at  $0.55 \mu\text{m}$  and an internal vertical distribution model (that may be overridden by user input). The default vertical profile of

aerosol particle density, shown in Fig. 4, is as specified by McClatchey et al. (1972). These models are meant to model the vertical distribution of aerosol particles in low ( $V = 5 \text{ km}$ ) and high visibility ( $V = 23 \text{ km}$ ) conditions. The vertical profiles of the 5- and 23-km visibility models are the same above 5-km altitude, but below that altitude, where most of the extinction occurs, they follow exponential profiles with differing density scale heights of 0.99 and 1.45 km for 5- and 23-km visibility, respectively. A weighted average of these vertical distribution models is used when an intermediate value of visibility is selected. For a horizontal path, the meteorologic visibility is defined as  $3.912/\sigma_{ext}$ , where the numeric factor is the natural logarithm of a 2% visible contrast threshold and  $\sigma_{ext}$  is the extinction coefficient (per kilometer) at the surface. Hence, since extinction is proportional to aerosol particle density, the vertical profile of aerosol optical depth is

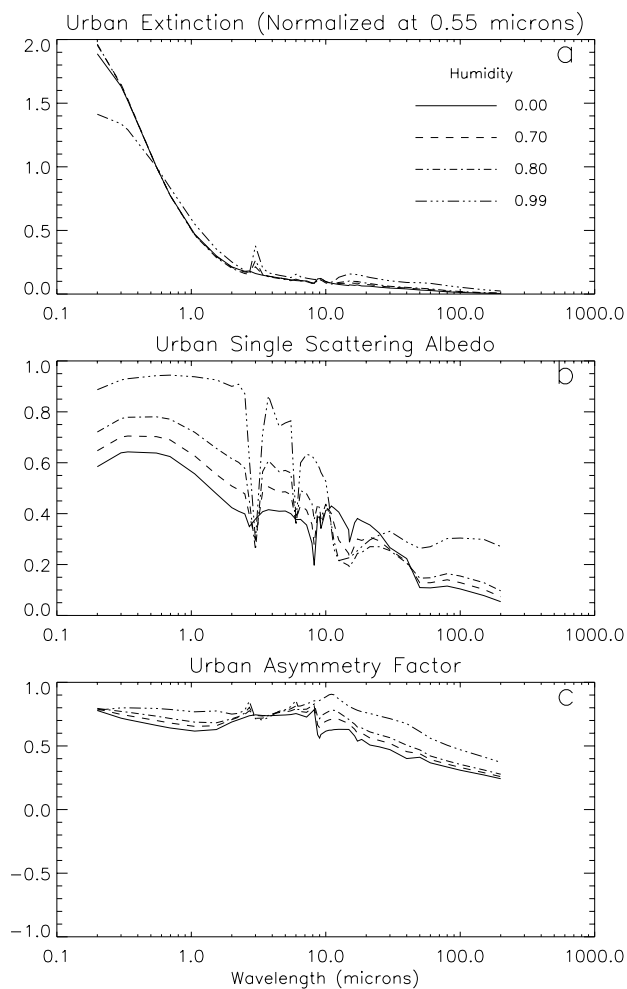


FIG. 2. Extinction efficiency (a), single-scattering albedo (b), and asymmetry factor (c) for urban aerosols.

$$\tau_{\text{aer}}(z) = \frac{3.912}{V} \int_z^{\infty} \frac{n(z)}{n(0)} dz, \quad (2)$$

where  $n(z)$  is the vertical profile of the aerosol particle density,  $V$  is the visibility in kilometers, and the upper-integration limit actually stops at the top of the atmospheric grid, 100 km.

In addition to the low-altitude aerosol models discussed above, SBDART also includes models for upper-atmospheric aerosols. Up to five aerosol layers can be specified (i.e., at five different altitudes), with radiative characteristics that model fresh or aged volcanic, meteoric, and upper-tropospheric background aerosols.

#### f. Rayleigh scattering

When an electromagnetic wave impinges on an object significantly smaller than its wavelength, a

time-varying electric dipole moment is induced in the object. Hence, the object becomes a new point source of dipole radiation. This redirection of wave energy is called Rayleigh scattering. Rayleigh scattering by gas molecules is responsible for many commonly observed phenomena in the SW spectrum, including blue skies and red sunsets. In terms of the wavelength  $\lambda$ , the Rayleigh scattering coefficient  $\sigma$  is given by (Liou 1980)

$$\sigma = \frac{8\pi^3(m^2 - 1)^2(6 + 3\delta)}{3\lambda^4 N^2(6 - 7\delta)}, \quad (3)$$

where  $m$  is the index of refraction of air,  $N$  is the number density of molecules, and  $\delta$  is the depolarization factor. Since the index of refraction varies with wavelength, the wavelength dependence of the scattering coefficient is slightly different from the simple and familiar  $\lambda^{-4}$  power law. Using results from the theory of dispersion of electromagnetic waves to relate  $m$  to  $N$  and using a depolarization factor of 0.0279, the Rayleigh optical depth (Shettle et al. 1980) is given by

$$\tau_{\text{ray}}(z) = (938\lambda^4 - 10\lambda^2)^{-1} \int_z^{\infty} \frac{N(z)}{N(0)} dz, \quad (4)$$

where the altitude  $z$  is the altitude in kilometers and the wavelength  $\lambda$  is in microns.

#### g. Discrete ordinate radiative transfer

The radiative transfer equation is numerically integrated with DISORT (Discrete Ordinate Radiative

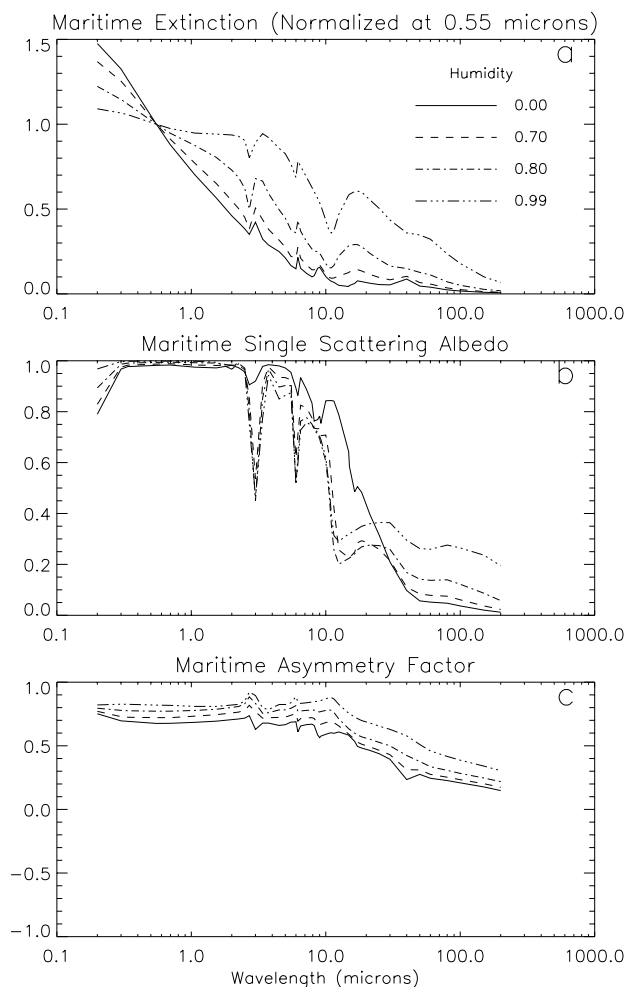


FIG. 3. Same as Fig. 2 but for maritime aerosols.

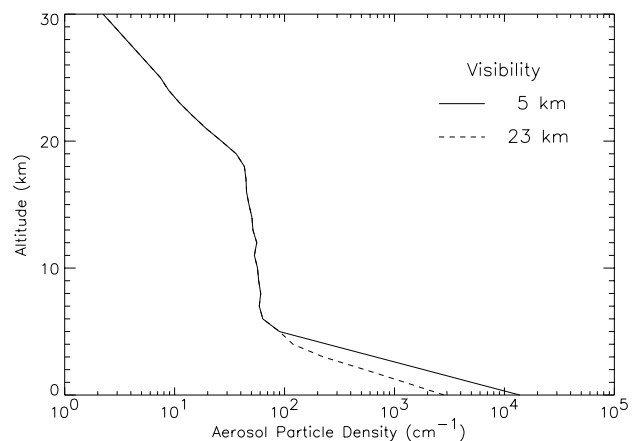


FIG. 4. Vertical profile of boundary layer aerosols for 23 (dashed) and 5 km (solid) visibility.

Transfer; Stamnes et al. 1988). The discrete ordinate method provides a numerically stable algorithm to solve the equations of plane-parallel radiative transfer in a vertically inhomogeneous atmosphere. The intensity of both scattered and thermally emitted radiation can be computed at different heights and directions. SBDART is configured to allow up to 50 atmospheric layers and 20 radiation streams (20 zenith angles and 20 azimuthal modes). Polarization effects are not included in SBDART.

The DISORT module was designed to treat plane-parallel radiative transfer. It is difficult to specify exact conditions for which the plane-parallel assumption is valid. However, in general, the horizontal transport of radiation should be unimportant when the scale of horizontal variability is very large compared to a relevant vertical scale. For example, when considering radiative transfer through stratus clouds, it would be reasonable to require homogeneous conditions over a horizontal distance about 10 times the cloud-base height (Ricchiazzi and Gautier 1998). When modeling the surface irradiation in clear-sky conditions, the horizontal distance scale is set by the vertical scale of the dominant scattering process. Hence, homogeneity over a larger horizontal scale is required when the optical depth of stratospheric aerosols is significant and greater than that of Rayleigh scattering or low-level aerosols.

DISORT uses a flat-earth coordinate system. In general this assumption is valid when the region of interest has a vertical extent much less than the radius of earth. This is generally the case when dealing with common sources of scattering in the earth's atmosphere. However, gas absorption can be important even at very high altitudes (e.g., UV absorption by stratospheric ozone). When considering large solar zenith angles, the flat-earth assumption may lead to significant errors. In our treatment of radiative transfer we have implemented a first-order correction, which computes the direct beam attenuation using the correct spherical geometry. This approach provides a much better estimate of the solar input into the lower atmosphere. Dahlback and Stamnes (1991) showed this approximation provides adequate estimates of atmospheric photolysis even for solar zenith angles as large as  $90^\circ$  when used with a plane-parallel radiative transfer model. SBDART does not contain corrections for refractive effects, but these effects are small for solar zenith angles less than about  $85^\circ$ . (At a solar zenith angle of  $85^\circ$  refractive effects extend the path length from 100-km altitude to the surface by only 1.4%.)

The input quantities required by DISORT include the solar spectral input, extinction optical depth, single-scattering albedo, and angular phase function of the scattered radiation. The extinction optical depth for each layer is the sum of the layer optical depths due to molecular absorption, aerosols, clouds, and Rayleigh scattering. Since the gas transmission at a particular wavelength is itself broken into a sum of three exponential terms, the complete solution to the multiscattering radiative transfer involves three separate invocations of the DISORT algorithm to treat each of the k-distribution components. Each subcalculation uses the same optical properties of clouds, aerosols, and Rayleigh scattering but different gas optical depths. A fraction of the solar input is assigned to each of the three k-distribution terms, with all the fractions summing to one.

In LOWTRAN's treatment of multiple scattering, the k-distribution weighting factors are specified as altitude-dependent parameters rather than the constant factors generally used in the k-distribution approach. In this way LOWTRAN can be used to model radiative heating rates for different altitudes in the atmosphere that may be radiatively dominated by the opacity of different molecular species. Due to the requirements of the DISORT subroutine, we have had to eliminate this flexibility. To use the LOWTRAN k-distribution parameters with DISORT we have computed vertically averaged factors weighted by the layer opacity. Though this simplification will tend to decrease the ability to model spectral regions for which opacity is dominated by different species at different altitudes, the overall error is probably small. As shown in section 2, the results obtained using this assumption agree well with the clear-sky longwave spectroscopic measurements.

The effective single-scattering albedo and asymmetry factor for a given atmospheric layer is taken to be the average of either quantity weighted by the opacity of each constituent (gas, aerosol, cloud, Rayleigh) within the layer. The asymmetry factor is used to generate a scattering phase function through the Henyey-Greenstein approximation. The Henyey-Greenstein parameterization provides good accuracy when applied to radiative flux calculations (van de Hulst 1968; Hansen 1969), but it is probably less reliable for radiance computations. While the DISORT model can treat more detailed phase function information, it is currently not practical to implement a more detailed model due to the lack of quantitative information on aerosol scattering properties.

### 3. Validation of the model with observations

#### a. Longwave comparisons

Since the mid-1980s the ICRCCM (Intercomparison of Radiation Codes used in Climate Modeling) working group has made an ongoing effort to establish a reference standard against which to compare radiation models. The earliest results from this program concentrated on the validation of longwave (LW) radiation models. Since reliable LW datasets were difficult to obtain, the initial goal was to compare models with state-of-the-art line-by-line (LBL) radiative transfer codes. Since LBL models do not make any spectral averaging assumption, these models should have the highest fidelity to the radiative processes in the atmosphere.

The results of this first round of intercomparisons revealed rather large discrepancies between different radiation codes (Luther et al. 1988). Worse yet, there were also distressingly large differences between different LBL models. Since that time LBL modelers have greatly upgraded their models, mainly by improving the treatment of water vapor continuum and providing a better partition of the absorption profile between algorithms for line cores and continua (Clough et al. 1992). Their efforts have filtered down to the low-resolution models on which LOWTRAN and SBDART are based.

The disappointing results from the first round of intercomparisons also spurred the community to develop SPECTRE (Spectral Radiation Experiment; Ellingson and Wiscombe 1996). The goal of this comprehensive measurement program was to establish observational standards used to test radiative transfer models. To achieve this objective, the design of SPECTRE followed from a careful consideration of how to minimize uncertainties due to radiometric calibration errors and emission by optical elements and gases in the optical path. In addition, uncertainties in the aerosol, humidity, and temperature profiles were reduced through in situ and remote sensing measurements during the observational periods.

As part of a new round of model comparisons based on SPECTRE results, the ICRCCM group members were provided with atmospheric state data and spectroscopic observations obtained at Coffeyville, Kansas, during November and December 1991. The spectral data were obtained with AERI (Atmospheric Emitted Radiance Interferometer), a Fourier transform spectrometer designed and operated by the University

of Wisconsin. Figure 5a shows results for a clear-sky observation made during conditions that were cool, dry, and relatively free of aerosols. This sample case is a good test of SBDART. Compared to a moister air column, the LW radiation emitted by a dry atmosphere is more sensitive to ambient conditions over the entire vertical column. In addition, the reduced water vapor opacity increases the importance of other molecular species that emit in the window region, thereby providing a test of how well SBDART simulates their emission.

In the comparison shown in Fig. 5b, the observations were degraded to SBDART's resolution by convolution with a square response function of width  $20\text{ cm}^{-1}$ . The overall agreement is very good. The degraded data are usually within  $5\text{ mW cm}^{-2}\text{ sr}^{-1}$  throughout the window region. Part of the discrepancy at  $600\text{ cm}^{-1}$  may be explained by the decreased sensi-

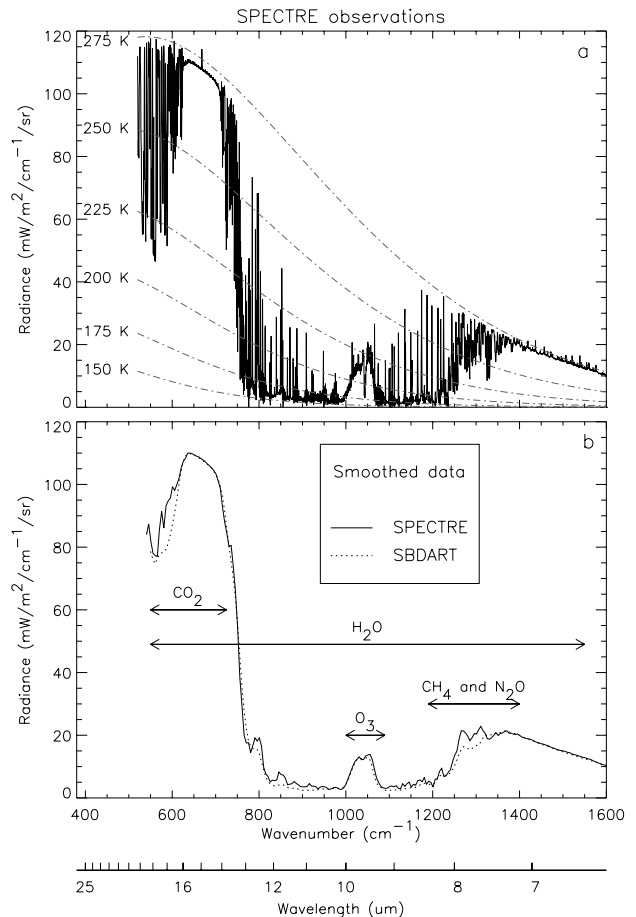


FIG. 5. (a) Observed spectra from AERI under cool-dry conditions. The dashed lines indicate blackbody radiation curves for a range of temperatures between 150 and 275 K. (b) AERI spectra smoothed with a  $20\text{ cm}^{-1}$  boxcar average (solid) compared to SBDART results (dotted).

tivity of the interferometer at longer wavelength. The spectral integration of this data from 600 to 1600  $\text{cm}^{-1}$  agrees with the SBDART prediction to within 3%, which is about three times as large as the calibration accuracy of the instrument. We have obtained similar results in clear-sky comparisons with the AERI deployed at the Southern Great Plains (SGP) observational site of the Atmospheric Radiation Measurement (ARM) program (Stokes and Schwartz 1994). The discrepancy between our model predictions and AERI appears to be a limitation in the SBDART model. Comparisons of the integrated AERI spectra with detailed line-by-line radiation model (e.g., Clough et al. 1992) typically show 1% agreement, even including the additional uncertainty introduced by the atmospheric state measurements.

Clearly, SBDART is not the correct tool for detailed analysis of AERI data in clear-sky conditions. However, it does provide quick estimates of wideband IR irradiance. By comparison, with more detailed models over a representative range of atmospheric conditions, it may be possible to develop correction factors to make these estimates both quick and accurate. It should also be noted that the discrepancies in downwelling irradiance between SBDART and more detailed models are much smaller when clouds are present. In this case SBDART correctly predicts a radiation spectrum in the window region characterized by blackbody emission at the cloud-base temperature. A more challenging test would be provided by a case with high, thin cirrus clouds. However, the radiative properties and microphysical description of clouds composed of ice or water-ice mix is not yet known well enough to sufficiently constrain the model.

#### *b. Shortwave comparison*

In some ways it is more difficult to validate the accuracy of a radiative transfer model in the SW than at longer wavelengths. At visible wavelengths clouds produce large variations in transmission over the typical range of cloud optical thickness. It is currently extremely difficult to constrain models with accurate estimates of cloud optical depth and microphysics. Even under clear skies, the uncertainty of atmospheric state, particularly aerosol turbidity, produces significant variation in the SW predictions, at a level much greater than would be present in the LW case. It is therefore essential to obtain along with the surface SW measurements, a set of high-quality atmospheric observations that include information on aerosol visibility over the SW spectral range. Such high-quality data

have been made available from the recently completed ARM SW Intensive Observation Period conducted in the fall of 1997.

To determine how well SBDART predicts total SW surface irradiance, we compared its predictions to observations made by the Baseline Surface Radiation Network (BSRN) at the SGP Central Facility. The BSRN dataset contains measurements from several SW and LW radiometric instruments. We used information from a shaded Eppley Precision Spectral Pyranometer (PSP) and an Eppley Normal-Incidence Pyrheliometer (NIP) to obtain the diffuse and direct SW radiation, respectively. The total SW irradiance was reconstructed by adding the diffuse irradiance to the product of the direct-normal irradiance and the cosine of the solar zenith angle. This reconstructed total irradiance is more accurate than can be obtained from an unshaded pyranometer because it bypasses the uncertainties of the instrument's cosine response (Kato et al. 1997). The passband of both the PSP and NIP is 290–2800 nm. Figure 6a,b shows a comparison of total and diffuse SW irradiance predicted by SBDART and observed by the BSRN on 30 September 1997. This day was very clear, with very low aerosol levels and no hint of clouds in the SW time history. As discussed below, the model calculations were run with both a "typical" weakly absorbing aerosol with a single-scattering albedo of 0.9 (Fig. 6a) and a strongly absorbing aerosol with a single-scattering albedo of 0.5 (Fig. 6b). All SBDART simulations used four radiation streams.

The data used for this comparison were combined from several ARM experiments. Meteorological information (vertical profiles of pressure, temperature, and relative humidity) was obtained from radiosondes, which were launched from the central facility several times during each day. Since total precipitable water is an important determinant of total SW, we used observations from the ARM Microwave Radiometer (that were available for afternoon hours only) to verify that vertical integration of water vapor profiles from the radiosondes agree to within a few percent of the microwave estimates. Using observations from either source, total water vapor path remained fairly constant at about 2  $\text{g cm}^{-2}$  throughout the day. The total column ozone used in the SBDART computation was set at 275 dobson units, which was the midday value measured by the Total Ozone Mapping Spectrometer instrument on the Earth Probe Satellite.

The Langley method (Harrison and Michalsky 1994) was used with observations from the Multifilter

Rotating Shadowband Spectrometer (MFRSR) to estimate optical depth within narrow (10 nm) passbands at 414, 499, 609, 665, and 860 nm. Aerosol optical depths were derived by subtracting out the known effects of Rayleigh scattering and ozone absorption in the Chappuis band, resulting in aerosol optical depths of 0.109, 0.083, 0.062, 0.053, and 0.044 at the aforementioned wavelengths. These values were extremely stable, with morning and afternoon regressions agreeing to within a few percent. Logarithmic interpolation (or extrapolation for  $\lambda < 414$  nm or  $\lambda > 860$  nm) was used to supply SBDART with aerosol optical depths covering the entire wavelength range of the calculation (290–2800 nm). Measurements from tower-mounted up- and down-looking MFRSRs provided spectral surface albedo near the central facility (Michalsky 1998, personal communication).

As shown in Fig. 6a, when a typical “rural” aerosol single-scattering albedo and asymmetry factor ( $\omega = 0.9$  and  $g = 0.8$ ) are assumed, the SBDART prediction of total irradiance is about 15–20  $\text{W m}^{-2}$  greater than the total observed SW. This discrepancy is roughly consistent with the 3% calibration accuracy of the instruments. SBDART’s prediction of direct SW irradiance (not shown) is within about 1% of the NIP observations. This last result can be considered a validation of both SBDART’s solar and gas absorption models and the accuracy of the narrowband optical depth retrievals.

A bit harder to explain is why SBDART overestimates the diffuse SW by almost 30% ( $25 \text{ W m}^{-2}$ ). Comparisons with observations on other days show a similar overestimate of the diffuse radiation. A potential source for this discrepancy may be an incorrect choice of aerosol scattering parameters. To check this possibility we repeated the SBDART simulation with an aerosol single-scattering albedo of 0.5, keeping the asymmetry factor at 0.8. These input values decreased the predicted diffuse radiation to a level within a few percent of the observations (Fig. 6b). A similar improvement can be obtained by fixing the single-scattering albedo at 0.9 and lowering the asymmetry factor to 0.1 (not shown). Though the scattering properties of aerosols are difficult to determine precisely, such small values of single-scattering albedo or asymmetry factor seem

inconsistent with in situ observations, which suggest that the primary constituent is mineral aerosol. SBDART’s overestimate of clear-sky diffuse radiation is consistent with comparisons performed by Kato et al. (1997), and may support their contention that current radiative transfer models neglect an important continuum absorption process at visible wavelengths.

We have also compared SBDART to measurements made with an accurately calibrated narrowband radiometer system deployed at Palmer Station, Antarctica (Ricchiazzi et al. 1995). We were able to achieve about 3% agreement with measurements of total (direct + diffuse) irradiance at 410 and 630 nm under clear skies. These observations were obtained under conditions of very low aerosol loading, for which assumptions regarding aerosol properties are less important. Unfortunately, the instrument used in this study did not provide a separate measurement of diffuse radiation.

#### 4. Web computation

To facilitate and promote the use of SBDART by a variety of investigators or instructors not necessarily familiar with computer programming, we have developed an extremely easy-to-use version for use on

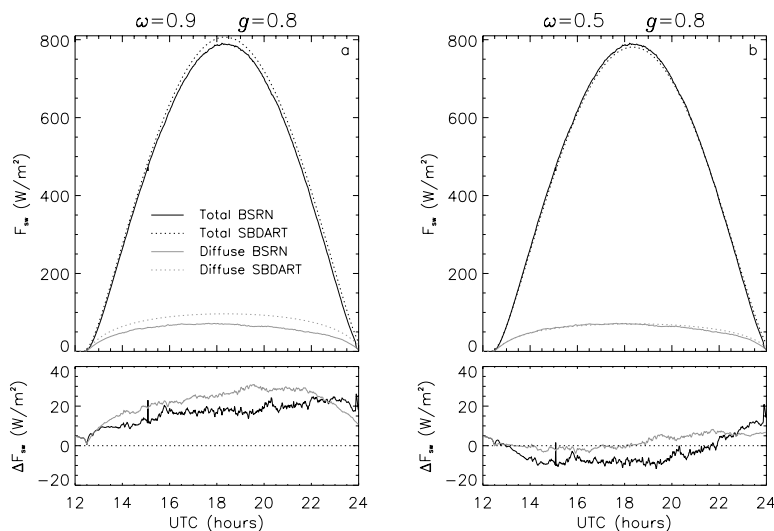


FIG. 6. (a) Total and diffuse irradiance for 30 September 1997 observed by the BSRN (solid) and predicted by SBDART (dashed). The SBDART calculation used aerosol optical depths derived from a Langley analysis of the MFRSR observations for the same day. The aerosol single-scattering albedo and asymmetry factor were set to 0.9 and 0.8, respectively. The difference, SBDART – BSRN, is shown in the lower panel for the total (solid) and diffuse (gray) component. (b) Same as Fig. 6a except the SBDART simulation used a aerosol single-scattering albedo of 0.5.

the World Wide Web. Through the use of a simple graphical user interface (GUI) anyone may carry out calculations spanning most of SBDART's capabilities without cost, detailed knowledge of the code, or formality. Our goals in doing so include both education and research. The Web version of SBDART has been found useful as a tool for assigned homework in graduate courses involving atmospheric radiation transfer or climate change. Perhaps this could be extended to undergraduate or even high school students. However, to date most use of the Web SBDART has been by research scientists who lack the resources or inclination to develop or implement their own radiation transfer code, or who wish to test SBDART before installing it. The Web version of SBDART has found use as a check on field measurements in real time, as an aid in design of satellite borne instruments, and as an analysis tool for atmospheric radiometric data.

At present, three types of calculations can be carried out through the GUI: broadband radiance, and spectral and broadband irradiance. The user chooses from various options for these calculations, replacing default values for such parameters as solar zenith angle, instrument filter function, atmosphere and aerosol models, etc. Custom input forms present the user with only those choices necessary for the calculation desired. One of these forms is illustrated in Fig. 7.

Any of the six U.S. standard atmospheres listed earlier may be chosen and, if desired, modified by a number of rawinsonde measurements taken at the ARM central site near Lamont, Oklahoma, during flight periods of the ARM Unmanned Aerospace Vehicle (the ARM-UAV) program.

Up to five layers of clouds are allowed, each specified by four parameters: altitude in integral kilometers, effective droplet radius, optical depth, and phase (if ice, then the effective radius is set to 106  $\mu\text{m}$ ).

A number of standard instrument response functions are available for choice by the user, including some from the National Oceanic and Atmospheric Administration's Advanced Very High Resolution Radiometers, and some from radiometers used by the ARM-UAV program (Valero et al. 1982). Alternatively, the user may specify an instrumental filter function that is flat between arbitrary wavelengths.

For broadband and spectral calculations, the user may specify the solar zenith angle (degrees), in which case the yearly average solar constant is used (Neckel and Labs 1984), or may specify a location, date, and time, in which case solar zenith angle and instantane-

ous value of the solar constant modified by earth-sun distance is used.

Radiance calculations require additional input to specify the zenith and azimuth angles for which radiance information is computed. These angles specify the direction of the propagating radiation. For example, zenith angle of 0° or 180° represents radiation propagating vertically up or down. The azimuth angle is measured clockwise from the horizontal projection of the sun's direct beam (0 is toward the forward scattering peak), as illustrated in Fig. 8. Results from these calculations are presented in the form of tables or graphics.

## 5. Conclusions

In this paper we have described SBDART, a newly available software tool for plane-parallel radiative transfer in the earth's atmosphere. Because of its relative ease of use and modular design, it should have widespread use in the geoscience community, as a research code, an educational tool, and a basis for the construction of new radiative transfer applications.

FIG. 7. Web user interface to SBDART.

Over the past few years, SBDART has been successfully used in a number of research efforts by us and other researchers (Lubin et al. 1994; Ricchiazzi et al. 1995; Koskela et al. 1996).

We anticipate that the Web version will be tested over a broader range of applications than we alone can provide. We hope the resulting user feedback will help us expedite the process of model improvement. We also hope its release will encourage other geoscience researchers to share their software tools with the community. In the mean time we solicit suggestions for improvements in the implementation or presentation of the Web version of SBDART at [sowle@mrcsb.com](mailto:sowle@mrcsb.com).

*Acknowledgments.* This work was supported in part by the Atmospheric Radiation Measurement Program of the U.S. Department of Energy under Grant 96ER61986, and in part by the National Science Foundation under Grant OPP9317120. The de-

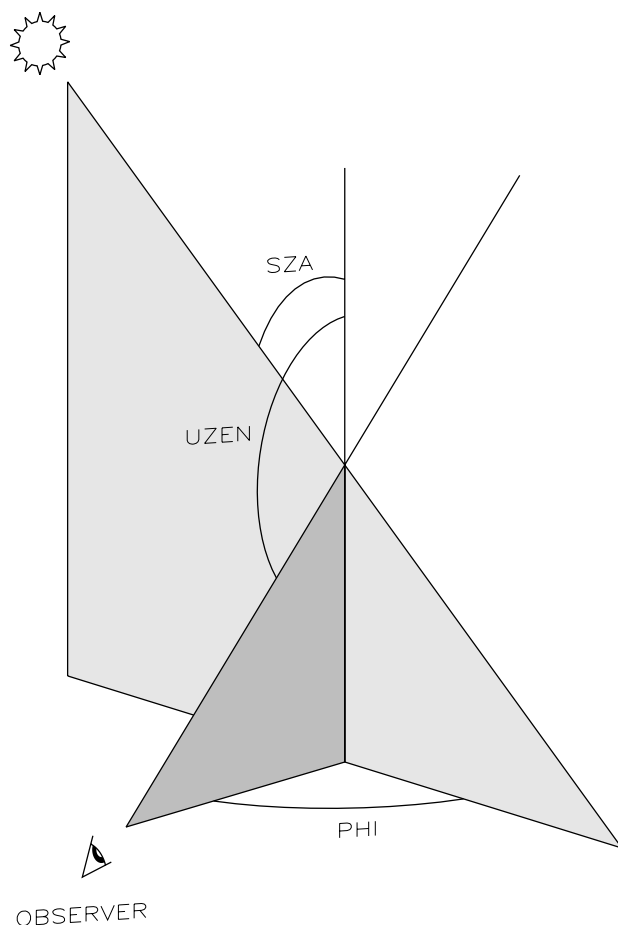


FIG. 8. The solar and viewing geometry of a SBDART radiance calculation is specified by the solar zenith angle (SZA), the viewing zenith angle (UZEN), and the relative azimuth angle (PHI).

velopment of the Web version of SBDART was sponsored by the ARM-UAV Program under Grant 94ER61820.

## Appendix: Operational features and examples

SBDART is provided as a self-contained FORTRAN 77 source code. Extensive input documentation is included in the release package. Minimum system requirements for a stand-alone installation are a FORTRAN compiler and 2.2 MB of free disk space. While running, SBDART uses about 2.3 MB of memory. SBDART has been successfully compiled and run with UNIX operating system on DEC and sun workstations, and with Windows NT using the FORTRAN PowerStation compiler. The time required to complete an SBDART simulation depends on the number of radiation streams used to resolve the angular radiance distribution and the number of quadrature points used to resolve the spectral range. For example, the computation of total SW (290–4000 nm) using 5 nm spectral resolution and four radiation streams takes about 40 s on a Pentium Pro 200 MHz system.

User directives to SBDART are handled with FORTRAN NAMELIST input. Though NAMELIST input is not part of the FORTRAN 77 standard, it is an extremely common extension available on most modern FORTRAN compilers and is part of the FORTRAN 90 standard. A significant advantage of NAMELIST input is that not all elements of an input block need be specified by the user. This makes SBDART fairly easy to learn. Since most of the code inputs have been initialized with reasonable default values, a new user can quickly learn how to use the code, concentrating first on specifying just a few interesting input parameters.

The SBDART input file is named INPUT. If this file is not found in the current working directory when SBDART is executed, the program will create it, filling in default values of all the NAMELIST parameters. The input file consists of two NAMELIST blocks *\$input* and *\$dinput*. Parameters in the *\$dinput* block relate to operating details of the DISORT radiative transfer module, while those in *\$input* are more general parameters that specify such things as the model atmosphere, the wavelength range, and output quantity options. Online documentation is provided which fully describes SBDART's input parameters. In the next section we present two sample input files and their respective outputs.

a. Example 1

This input file directs SBDART to compute the downwelling spectral surface irradiance from 0.25 to 1.0  $\mu\text{m}$ :

```

$input
WLINF      =      0.25,
WLSUP      =      1.0,
WLINC      =      0.005,
IDATM      =      4,
IOUT       =      1,
$end
    
```

The input quantity WLINC controls the spectral resolution of the calculation. In this example the step size is set to 0.005  $\mu\text{m}$ . The input quantity IDATM specifies a model atmosphere, in this case the subarctic-summer model. Setting the input parameter IOUT = 1 indicates that spectral output is desired. Nearly 60 model parameters and a dozen output options may be specified in the input file. However, as shown in this example, because the code is initialized with reasonable default values, a new user can obtain meaningful output by specifying only a few inputs.

Graphical output produced by this input file is shown in Fig. A1. The spectral detail obtained in this example is somewhat less than the maximum available. SBDART allows the spectral step size to be specified in constant increments of wavelength, wavenumber, or log of wavelength. To take full advantage of the spectral resolution of the molecular band-models and solar constant tables within SBDART, the spectral step interval should be set at 20  $\text{cm}^{-1}$ . This results in 10 times better resolution than shown in the

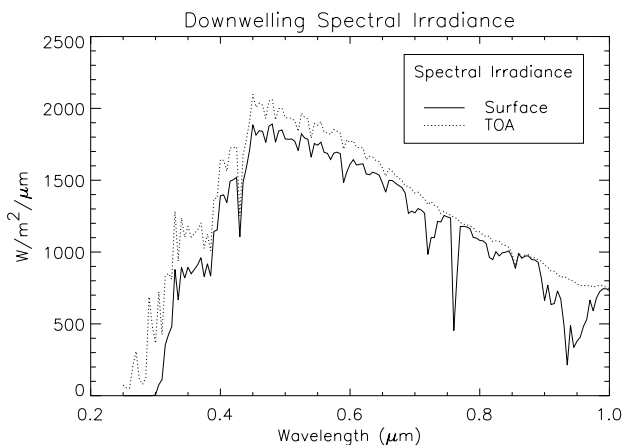


FIG. A1. SBDART results for spectral surface irradiance at the top of the atmosphere (dotted) and at the surface (solid).

figure, but at the cost of 10 times greater execution time.

b. Example 2

This input file causes SBDART to compute top of atmosphere (TOA) radiance at 0.55  $\mu\text{m}$ :

```

$input
WLINF      =      0.55,
WLSUP      =      0.55,
IDATM      =      1,
ISALB      =      4,
SZA        =      60,
ZCLOUD     =      1,
TCLD       =      5,
IOUT       =      23,
$end
$dinput
NSTR       =      16,
NZEN       =      16,
UZEN       =      0,15,32,45,60,70,80,89,91,
            100,110,120,135,148,165,180
NPHI       =      13,
PHI        =      0,15,30,45,60,75,90,105,
            120,135,150,165,180,
$end
    
```

In this example the solar zenith angle is set to 60°, the cloud height is 1 km, and the cloud optical depth is 5. An ocean surface (ISALB = 4) and a tropical atmosphere are assumed (IDATM = 1). Radiance output is obtained by specifying IOUT = 23. The number of viewing zenith and azimuth angles is set by parameters NZEN and NPHI, respectively, while the parameters UZEN and PHI specify zenith angles and relative azimuth angles at which the radiance information is generated (see Fig. 8). In the previous example, the input parameter NSTR, which sets the number of internal radiation streams, was left at its default value of 4 (four polar angles and four azimuthal modes). While four streams are adequate for irradiance computations (irradiance predictions with NSTR = 4 are within a percent of calculations performed with a greater number of streams), radiance predictions require more streams to better resolve the angular dependence of the radiation field. As a result, given the same wavelength integration interval, the calculation of radiance takes much longer than irradiance.

Figure A2a shows contour plots of TOA and surface radiance produced by this sample file. A similar case with a cloud optical depth of 10 is shown in

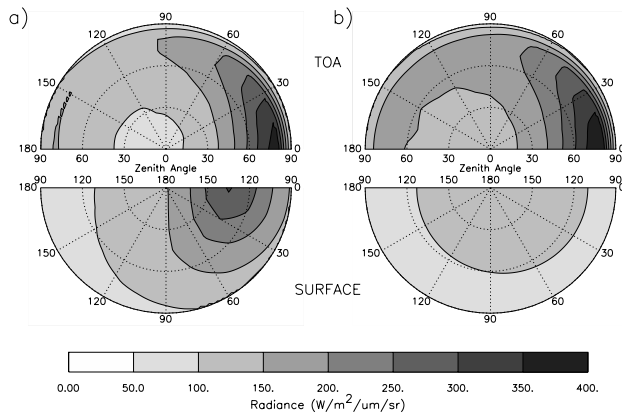


FIG. A2. (a) Radiance distribution at TOA (upper semicircles) and at the surface (lower semicircles) for the SBDART model run specified in example 2, that is, cloud optical depth 5, cloud height 1 km, and solar zenith angle  $60^\circ$ . (b) Same as fig. 5a, but for a cloud optical depth 10.

Fig. A2b. The horizontal axis of each semicircle denotes the zenith angle of propagating radiation, with upwelling directed radiation shown in the upper panel and downwelling radiation in the lower. The outer edge of each semicircle represents rays propagating in nearly horizontal directions, while the central regions indicate rays traveling more nearly up or down. The relative azimuth angle is labeled at the outer edge of each semicircle. Since the radiance is symmetric with respect to relative azimuth, only the relative azimuth range from  $0^\circ$  to  $180^\circ$  is shown.

An interesting physical effect illustrated by this figure is the persistence of forward scattering through an optically thick cloud. In the optical depth 5 case, the photons emerging from the bottom of the cloud are directed predominately along the direct beam direction of  $120^\circ$  with respect to zenith. This is due to the strong forward scattering of cloud droplets. As the optical depth is increased to 10 and beyond, the “memory” of the original solar zenith angle is lost, the anisotropy of the radiance decreases, and the direction of maximum radiance approaches  $180^\circ$ .

## References

Berk, A., L. W. Bernstein, and D. C. Robertson, 1983: MODTRAN: A moderate resolution model for LOWTRAN 7. Rep. AFGL-TR-83-0187, 261 pp. [Available from Air Force Geophysical Laboratory, Hanscom Air Force Base, MA 01731-5000.]  
 Bernstein, L. S., A. Berk, D. C. Robertson, P. K. Acharya, G. P. Anderson, and J. H. Chetwynd, 1996: Addition of a correlated-

k capability to MODTRAN. *Proc. 19th Annual Conf. on Atmospheric Transmission Models*. Hanscom AFB, MA, 261 pp. [Available from Air Force Geophysical Laboratory, Hanscom Air Force Base, MA 01731-5000.]  
 Clough, S. A., M. J. Iacono, and J.-L. Moncet, 1992: Line-by-line calculations of atmospheric fluxes and cooling rates: Application to water vapor. *J. Geophys. Res.*, **97**, 761–785.  
 Dahlback, A., and K. Stamnes, 1991: A new spherical model for computing the radiation field available for photolysis and heating at twilight. *Planet. Space Sci.*, **39**, 671–683.  
 Ellingson, R. G., and W. J. Wiscombe, 1996: The Spectral Radiance Experiment (SPECTRE) - Project description and sample results. *Bull. Amer. Meteor. Soc.*, **77**, 1967–1985.  
 Hansen, J. E., 1969: Exact and approximate solutions for multiple scattering by cloudy and hazy planetary atmospheres. *J. Atmos. Sci.*, **26**, 478–487.  
 Harrison, L. C., and J. Michalsky, 1994: Objective algorithms for the retrieval of optical depths from ground-based measurements. *Appl. Opt.*, **33**, 5126–5132.  
 Kato, S., T. P. Ackerman, E. E. Clothiaux, J. H. Mather, G. G. Mace, M. L. Wesely, F. Murcray, and J. Michalsky, 1997: Uncertainties in modeled and measured clear-sky surface shortwave irradiances. *J. Geophys. Res.*, **102**, 25 881–25 898.  
 Kneizys, F. X., E. P. Shettle, W. O. Gallery, J. H. Chetwynd, L. W. Abreu, J. E. A. Selby, S. A. Clough, and R. W. Fenn, 1983: Atmospheric transmittance/radiance: Computer code LOWTRAN 6, Rep. AFGL-TR-83-0187, 200 pp. [Available from Air Force Geophysical Laboratory, Hanscom Air Force Base, MA 01731-5000.]  
 Kondratyev, K. Y., 1969: *Radiation in the Atmosphere*. Academic Press, 912 pp.  
 Koskela, T., A. Heikkilä, J. Damski, P. Taalas, and A. Kylling, 1996: UV-B radiation at common optical air masses: Geographical comparison and model performance tests. *Proc. Int. Radiation Symp., IRS'96: Current Problems in Atmospheric Radiation*, Fairbanks, Alaska, 925–929.  
 Liou, K.-N., 1980: *An Introduction to Atmospheric Radiation*. Harcourt Brace Jovanovich, 392 pp.  
 Lubin, D., P. Ricchiazzi, C. Gautier, and R. H. Whritner, 1994: A method for mapping Antarctic surface UV radiation using multispectral satellite imagery. *Ultraviolet Radiation in Antarctica: Measurements and Biological Effects*, C. S. Weiler and P. A. Penhale, Eds., American Geophysical Union Antarctic Research Series, American Geophysical Union, 53–81.  
 Luther, F., R. Ellingson, Y. Fouquart, S. Fels, N. Scott, and W. Wiscombe, 1988: Intercomparison of radiation codes in climate models (ICRCCM): Longwave clear-sky results. *Bull. Amer. Meteor. Soc.*, **69**, 40–48.  
 McClatchey, R. A., R. W. Fenn, J. E. A. Selby, F. E. Volz, and J. S. Garing, 1972: Optical properties of the atmosphere. 3rd ed. AFCRL Environ. Res. Papers No. 411, 108 pp.  
 Neckel, H., and D. Labs, 1984: The solar radiation between 3300 and 12500 Å. *Sol. Phys.*, **90**, 205–258.  
 O'Hirok, W., and C. Gautier, 1998: A three-dimensional radiative transfer model to investigate the solar radiation within a cloudy atmosphere. Part I: Spatial effects. *J. Atmos. Sci.*, **55**, 2162–2179.  
 Pierluissi, J. H., and G.-S. Peng, 1985: New molecular transmission band models for LOWTRAN. *Opt. Eng.*, **24** (3), 541–547.

- Reeves, R. G., A. Anson, and D. Landen, Eds., 1975: *Manual of Remote Sensing*. First ed. Amer. Soc. Photogrammetry, 2144 pp.
- Ricchiazzi, P., and C. Gautier, 1998: Investigation of the effect of surface heterogeneity and topography on the radiation environment of Palmer Station, Antarctica, with a hybrid 3D radiative transfer model. *J. Geophys. Res.*, **103**, 6161–6176.
- , —, and D. Lubin, 1995: Cloud scattering optical depth and local surface albedo in the Antarctic: Simultaneous retrieval using ground-based radiometry. *J. Geophys. Res.*, **100**, 21 091–21 104.
- Schwartz, S. E., 1996: The whitehouse effect—Shortwave radiative forcing of climate by anthropogenic aerosols: An overview. *J. Aeros. Sci.*, **27**, 359–382.
- Shettle, E. P., and R. W. Fenn, 1975: Models of the atmospheric aerosols and their optical properties. *AGARD Conf. Proc., Optical Propagation in the Atmosphere*, Lyngby, Denmark, NATO Advisory Group for Aerospace Research, 2.1–2.16.
- , F. X. Kneizys, and W. O. Gallery, 1980: Suggested modification to the total volume molecular scattering coefficient in LOWTRAN. *Appl. Opt.*, **19**, 2873–2874.
- Staetter, R., and M. Schroeder, 1978: Spectral characteristics of natural surfaces. *Proc. Int. Conf. on Earth Observation from Space and Management of Planetary Resources*, Toulouse, France, Council of Europe, Commission of the European Communities, and European Association of Remote Sensing Laboratories, 661 pp.
- Stamnes, K., S. Tsay, W. Wiscombe, and K. Jayaweera, 1988: Numerically stable algorithm for discrete-ordinate-method radiative transfer in multiple scattering and emitting layered media. *Appl. Opt.*, **27**, 2502–2509.
- Stokes, G. M., and S. E. Schwartz, 1994: The atmospheric radiation measurement (ARM) program: Programmatic background and design of the cloud and radiation test bed. *Bull. Amer. Meteor. Soc.*, **75**, 1201–1221.
- Tanre, D., C. Deroo, P. Duhaut, M. Herman, J. J. Morcrette, J. Perbos, and P. Y. Deschamps, 1990: Description of a computer code to simulate the satellite signal in the solar spectrum: The 5S code. *Int. J. Remote Sens.*, **11** (4), 659–668.
- Valero, F. P. J., P. J., Warren, J. Y. Gore, and L. P. M. Giver, 1982: Radiative flux measurements in the troposphere. *Appl. Opt.*, **21**, 831–838.
- , and Coauthors, 1997: Absorption of solar radiation by the cloudy atmosphere: Interpretations of collocated aircraft measurements. *J. Geophys. Res. Atmos.*, **102**, 29 917–29 927.
- van de Hulst, H. C., 1968: Asymptotic fitting, a method for solving anisotropic transfer problems in thick layers. *J. Comput. Phys.*, **3**, 291–306.
- Wiscombe, W. J., 1980: Improved Mie scattering algorithms. *Appl. Opt.*, **19**, 1505–1509.
- , and J. W. Evans, 1977: Exponential-sum fitting of radiative transmission functions. *J. Comput. Phys.*, **24**, 416–444.
- , and S. G. Warren, 1980: A model for the spectral albedo of snow. Part I: Pure snow. *J. Atmos. Sci.*, **37**, 2712–2733.
- Zhang, M. H., R. D. Cess, and X. D. Jing, 1997: Concerning the interpretation of enhanced cloud shortwave absorption using monthly-mean earth radiation budget experiment/global energy balance archive measurements. *J. Geophys. Res. Atmos.*, **102**, 25 899–25 905.

